Phase-lagged amplitude modulation of hemipelagic cycles: A potential tool for recognition and analysis of sea-level change

Jiří Laurin* Institute of Geophysics, Academy of Sciences of the Czech Republic, Boční II/1401, 141 31 Prague, Czech Republic
Stephen R. Meyers Department of Geology and Geophysics, Yale University, New Haven, Connecticut 06511, USA
Bradley B. Sageman Department of Geological Sciences, Northwestern University, Evanston, Illinois 60208, USA
Dave Waltham Department of Geology, Royal Holloway University of London, Egham, Surrey TW20 OEX, UK

ABSTRACT

Many ancient rhythmic hemipelagic sequences have been interpreted to record orbital variations, but the exact nature of the climatic and depositional transfer functions responsible for this link remains poorly understood. Two-dimensional numerical simulations were used to explore selected aspects of orbital signal distortion in linked siliciclastic and hemipelagic systems. The models suggest that transfer of multiorder (e.g., 20, 100, and 400 k.y.) oscillations in relative sea level into the hemipelagic record produces an inherent amplitude distortion of the shorter-period (e.g., 20 k.y.) cycle. This distortion gives rise to amplitude modulation (AM), which is qualitatively similar to AM of orbitally driven changes in insolation (e.g., eccentricity modulation of precession-driven cycles). However, unlike the orbitally driven AM, synthesized AM is distinctly phase shifted relative to the stratigraphic record of the long-period (e.g., 100 k.y., 400 k.y.) cycle as a result of sea-level–driven changes in the storage capacity of nearshore through alluvial parts of the source siliciclastic system. Hence, multiorder changes in sea level can leave a distinct AM signature in dilution-affected hemipelagic records, thus making hemipelagic rhythms due to eccentricity-forced sea-level changes distinguishable from other types of orbitally driven hemipelagic cyclicity.

Keywords: amplitude distortion, hemipelagic sedimentation, sea level, cycles, modeling, spectral analysis.

INTRODUCTION

Fourier techniques have been used to confirm the presence of orbital periodicities in many ancient rhythmic hemipelagic sequences. Although this provides strong support for the link between climate and hemipelagic sedimentation through processes such as sea-level– or sediment-supply–driven siliciclastic dilution and/or carbonate production, the nature of the link remains poorly understood. In particular, nonlinear processes inherent in the depositional transfer functions modify and distort primary orbital signals, but have received little attention. Ripepe and Fischer (1991) and Herbert (1994) are notable exceptions, but even these studies were restricted to one-dimensional model systems.

Here we use two-dimensional stratigraphic modeling to explore sea-level–driven cycles of siliciclastic dilution, and show that long-period signals (e.g., 100 k.y., 400 k.y.) produce systematic temporal variation in the amplitude (amplitude modulation, AM) of a relatively short period signal (e.g., 20 k.y.) because of the nonlinear character of the sea-level–sedimentation transfer function. The studied AM pattern is similar to the AM of the precession index observed in the insolation record (Fig. 1), except that it is distinctly phase

shifted relative to the record of the longer-period cycle. Although these depositional distortions make it difficult to quantify AM associated with the primary signal, they bear important information about the depositional forcing mechanisms. We propose that distinct phase-lagged AM patterns could be indicative of sea-level–forced cycles of siliciclastic dilu-
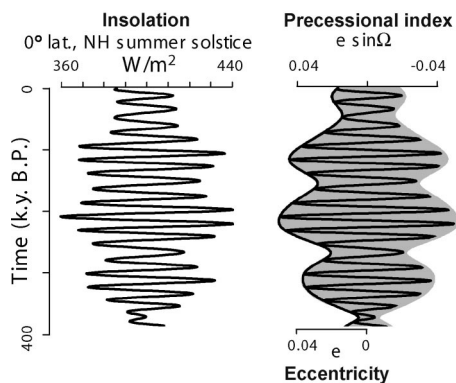
Figure 1. Example of amplitude modulation (AM) of climate forcings. Daily Northern Hemisphere (NH) summer solstice insolation at equator, precessional index, and orbital eccentricity for past 400 k.y. were calculated with Analyseries software (Paillard et al., 1996) using solution of Laskar (1990). Insolation is dominated by precession of equinoxes, whose amplitude varies with orbital eccentricity.

tion. Their presence in hemipelagic records can help to identify orbitally forced eustatic changes and thus contribute to our understanding of orbital-climate link in Earth history.

MODEL

Hemipelagic sedimentation was simulated with the SedTec2000 program for two-dimensional modeling of mixed carbonate-siliciclastic systems (Boylan et al., 2002). The siliciclastic sedimentation algorithm is adopted from Hardy and Waltham (1992). In deep water unaffected by erosion, this algorithm results in an exponentially decreasing sedimentation rate with distance. The rate at which the sedimentation decreases is controlled by a transport distance, which characterizes the typical distance traveled by sediments before deposition. Although user defined, the transport distances are generally short for coarse sediments and long for fine sediments (see GSA Data Repository).[1]

Representative model runs were designed to produce 10-km-scale transgressive-regressive oscillations in response to meter-scale changes in relative sea level and to generate a stratigraphic record composed of mixed siliciclastic-carbonate sediment, accumulating at a (compacted) rate of ~0.5 cm/k.y. between 300 and 500 km offshore from the model margin. The simulated depositional systems are comparable to epeiric depositional systems such as the Western Interior (USA) during the Cretaceous. Pelagic-carbonate production was set constant, i.e., not affected by changes in siliciclastic flux, to preclude amplitude distortion due to production changes. Similarly, carbonate dissolution in the water column and diagenetic changes were not modeled. This approach was adopted to explicitly isolate first-order signal distortions related to changes in siliciclastic flux.

Two runs—SIN 1 and SIN 2—demonstrate the ability of relative sea-level–driven siliciclastic-hemipelagic depositional systems to synthesize AM from signals with invariable amplitudes. The input relative sea level had

E-mail: laurin@ig.cas.cz
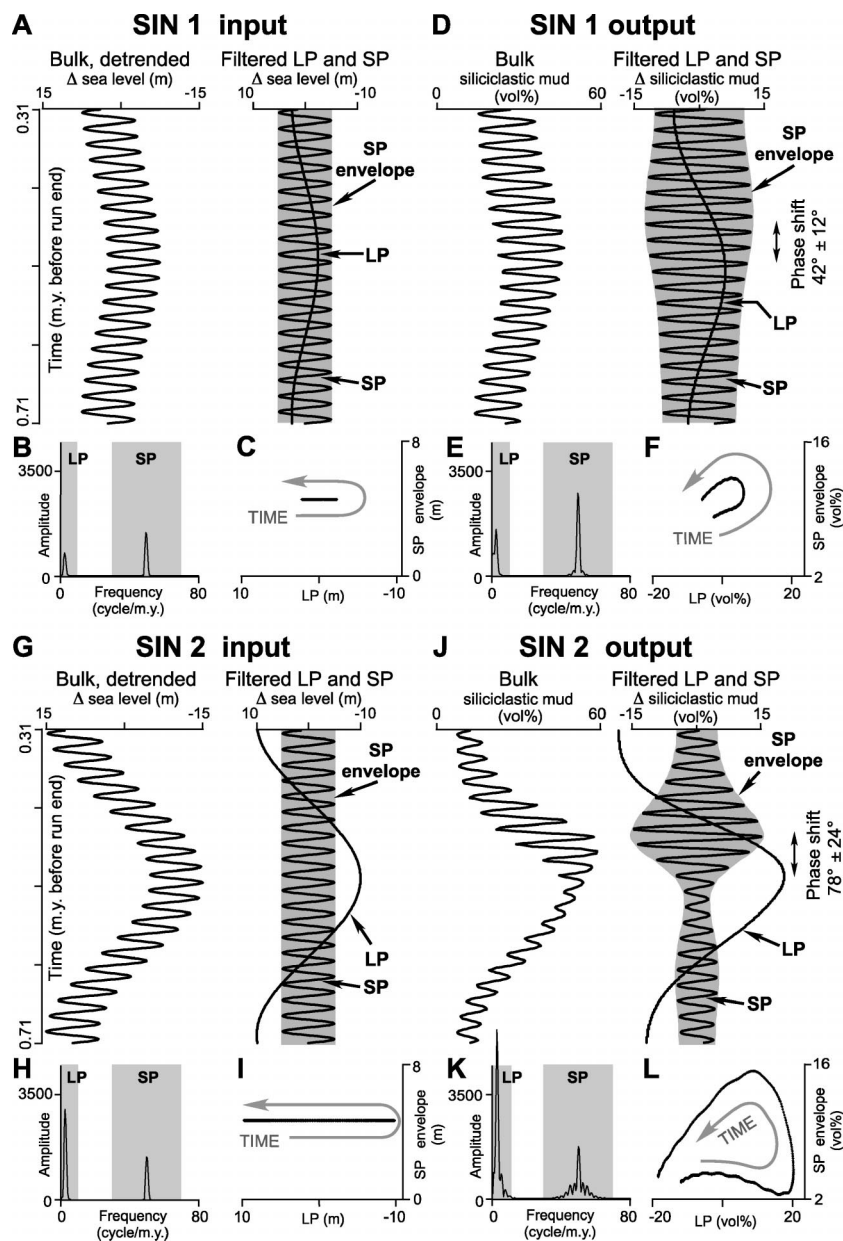
Figure 2. Selected input and output parameters of SIN 1 (A–F) and SIN 2 (G–L) models. Only portions of 1.2 m.y. model runs are shown (see footnote 1). A, G: Input signals are represented by 20 k.y. and 400 k.y. sinusoidal oscillations in relative sea level. B, H: Periodograms of input sea-level curves. C, I: Demodulated short-period (SP) cycles of input signals plotted against long-period (LP) components of input signals. Note that input SP amplitudes are invariable. D, J: Model output (vol% mud) plotted against time. For depth-domain output, see footnote 1. E, K: Periodograms of output (vol%) mud curves. F, L: Demodulated SP cycles of output signals plotted against LP components of output signals. Note that amplitude envelopes of output SP signals (grayed in D and J) differ from amplitude envelopes of input SP signals, and are distinctly (~42° and ~78°) phase shifted relative to output LP signals.

two orders of sinusoidal oscillation with a short period (SP) of 20 k.y. and a long period (LP) of 400 k.y. The amplitude of the SP cycle is 5 m in both model runs, whereas the amplitude of the LP cycle is low (2.5 m) in the SIN 1 model and high (10 m) in the SIN 2 model. Model output is displayed as volume percentage of siliciclastic mud in a compacted hemipelagic sediment 400 km from the model basin margin (Fig. 2).

The SIN models provide simple forcing scenarios generated to clearly illustrate potential amplitude distortion via the depositional system. Interference between this depositional-system–induced distortion and the inherent eccentricity modulation of precession amplitude is investigated in the MILex model herein. In this example, insolation series containing precession and obliquity (solution of Laskar, 1990; see Data Repository [footnote 1]) is lin-

early combined with orbital eccentricity (Laskar, 1990) to generate a composite sea-level curve. Although based on a simplistic sea level–climate transfer function, the enhancement of eccentricity power is in accordance with evidence from the paleoclimate record (e.g., late Quaternary: Imbrie et al., 1993; Cretaceous: Plint, 1991).

AM ASSESSMENT

The individual cyclic signals were extracted from the composite input sea-level curves and the output vol% mud curves by bandpass filtering (Gaussian window) the appropriate frequency ranges (determined by Fast Fourier Transform; Analyseries software: Paillard et al., 1996). The amplitude envelope (instantaneous amplitude) of the SP component was calculated with a Hilbert Transform by the program Arand (Howell, 2001). Finally, cross-spectral analysis performed with Arand was used to determine the phase of the LP signal relative to the SP amplitude envelope.

RESULTS

Both SIN runs produced distinct AM of the originally sinusoidal input SP signal by transforming it from sea-level oscillations to oscillations in offshore siliciclastic flux and hemipelagic lithology (Fig. 2). The synthesized model output SP amplitude envelopes are nearly identical in their wavelength to the input LP cycles, suggesting that the AM is forced by the LP sea-level cycle. This is supported by the fact that the degree of AM increases with an increase in the ratio of input LP vs. input SP amplitude (Fig. 2). In both models, the lowest output SP amplitudes form during fall and slow rise in LP relative sea level, whereas the highest amplitudes of the output SP cycle coincide with accelerated rise in LP relative sea level (Figs. 2 and 3). This scenario gives rise to a distinct (e.g., 40°–80°; Fig. 2) phase shift of the SP amplitude envelope of the output signal relative to the LP component of the output signal (Figs. 2D, 2J): both model runs generated the maximum SP amplitudes during decline in output LP values (Figs. 2F, 2L).

DISCUSSION

The simulations suggest that AM is inherent in oscillations of offshore siliciclastic flux that are governed by composite, sea-level–driven transgressions and regressions (T-R). In general, the maximum possible amplitude of shoreline T-R response to a unit oscillation in relative sea level depends on the topset slope and foreset height (Fig. 4): while the topset slope limits the width of topset area flooded during a unit relative sea-level rise and thus limits the magnitude of shoreline retreat, the foreset height affects the magnitude of the basinward shoreline advance (cf. Ross et al.,
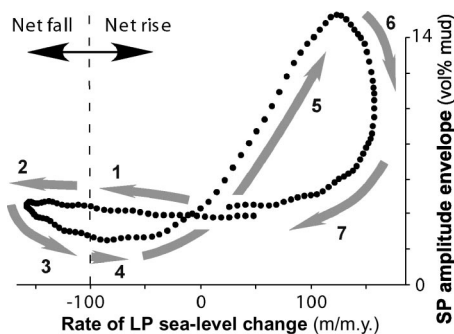
Figure 3. Demodulated short-period (SP) component of SIN 2 output vol% mud curve plotted against rate of change of long-period (LP) component of SIN 2 input sea-level curve. SP and LP sea-level oscillations (Fig. 2) were superimposed upon constant, 100 m/m.y. relative sea-level (RSL) rise (dashed line). Individual parts of plot are interpreted as follows (see text discussion and Fig. 4). (1) Net RSL rise decelerates: SP amplitude low, because foresets are high and shoreline is close to basin margin; SP amplitude increases slightly as shoreline migrates basinward upon unforced progradation. (2) RSL fall accelerates: SP amplitude low, but increases slightly as foresets become shallower; increasing topset slope (α; Fig. 4) suppresses SP amplitude. (3) RSL fall decelerates: SP amplitude decreases as topset width (TW; Fig. 4) is small, and foresets prograde into deeper water basinward of previous LP regressive system. (4) Net RSL starts rising: topset width starts increasing, but SP amplitude continues to decrease slightly, because foreset height increases upon shoreface aggradation. (5) Net RSL rise accelerates: SP amplitude increases as topset width increases, and foresets, nested atop previous regressive system, are shallow (Fig. 4). (6) RSL rise continues to accelerate, but SP amplitude drops as transgressive system approaches physiographic margin of basin and foreset height increases. (7) RSL rise decelerates: SP amplitude continues to decrease as topsets are restricted by physiographic margin of basin and foreset height continues to increase.

Figure 4. Conceptual model of sensitivity of transgression-regression (T-R) changes and changes in offshore siliciclastic flux to short-period (SP) relative sea-level oscillations in course of long-period (LP) relative sea-level cycle. LP relative sea-level changes produce systematic changes in foreset height (FH) and topset slope (α; TW = width of topsets flooded during SP relative sea-level rise). These changes in turn result in systematic changes in amplitude of SP, sea-level–driven T-R movements, and (assuming invariable hydraulic conditions) corresponding changes in offshore siliciclastic flux. Maximum SP amplitudes of siliciclastic flux (Max SP amp) form during rise in LP relative sea level and decline in LP siliciclastic flux. Thick lines—topsets; thin lines—foresets and bottomsets.

1995; Liu et al., 1998). The topset slope results from interplay of the alluvial gradients and the cross-sectional path of the migrating shoreline (shoreline trajectory; Helland-Hansen and Martinsen, 1996). Assuming constant hydraulic conditions and sediment flux, the foreset height depends on the seafloor morphology (Fig. 4). Both the topset slope and foreset height vary systematically with LP changes in relative sea level, giving rise to systematic changes in the amplitude of shoreline T-R response to SP oscillations in relative sea level (Fig. 4), as described here.

LP Relative Sea-Level Fall

Although complicated by the actual alluvial gradients, a forced-regressive topset typically establishes a relatively steep slope that approximates the shoreline trajectory (review in Helland-Hansen and Martinsen, 1996; Fig. 4).

After a previous episode of LP relative sea-level rise, the forced-regressive system progrades into a relatively deep marine basin (Fig. 4). In general, this arrangement suppresses the amplitudes of T-R movements and corresponding changes in offshore siliciclastic flux generated by the SP sea-level oscillations.

LP Relative Sea-Level Rise

Alluvial accumulation typically resumes landward of the shoreline, giving rise to a relatively gentle and wide topset zone (Fig. 4). Flooding of the topset area of the previous LP regressive system generates shallow foresets (Fig. 4). This arrangement promotes a high-amplitude T-R response to unit SP oscillations in relative sea level. The T-R amplitudes start decreasing as the continuing rise in relative sea level generates higher foresets and the shoreline approaches the physiographic basin margin (Figs. 3 and 4).

Phase Signature

The preceding relationships imply that T-R responses to SP (e.g., 20 k.y.) cycles in relative sea level reach their maximum amplitude during relative sea-level rise of the LP (e.g., 100 k.y., 400 k.y.) cycle. Any preexisting AM (e.g., eccentricity modulation of precession) will be deformed more or less strongly in this direction (Fig. 5). Because the LP cycle is relatively weakly distorted by transfer through the depositional system (Figs. 2D, 2J, and 5), the output signal tends to display a phase lag

between the SP amplitude envelope and the record of the LP cycle (up to 115°; Fig. 5). In sediment-supply–driven T-R cycles, widening of the topset area upon regression and narrowing of the topset area upon transgression should attenuate the effects of changing foreset height. Although distinct AM whose amplitude maximum coincides with LP decline in siliciclastic flux provides a signature of sea-level forcing of the LP siliciclastic-flux cycle, further work will be needed to resolve the full range of response to changes in sediment supply and sea level.

Model Limitations

This model does not simulate alluvial sedimentation. Therefore, it does not reproduce the response of nonmarine accumulation to changing base level and shoreline position, although the effect of high alluvial gradients near steep basin margins is partly mimicked (Fig. 3). Furthermore, nonlinearities inherent in carbonate production, dissolution, and diagenesis have not been addressed. Further simulations that use linked alluvial-marine systems and that incorporate production, dissolution, and diagenesis will refine our understanding of these depositional amplitude distortions.

CONCLUSIONS

Simulated examples are given of systematic, nonlinear distortions of periodic signals in linked siliciclastic and hemipelagic systems.

MILex input

Bulk, detrended Δ sea level (m)
Filtered ~20 k.y. Δ sea level (m)

MILex output

Bulk siliciclastic mud (vol%)
Filtered ~20 k.y. Δ siliciclastic mud (vol%)

Phase shift

Time (m.y. before run end)

~100 k.y., ~400 k.y. Δ sea level (m)

~100 k.y., ~400 k.y. Δ siliciclastic mud (vol%)
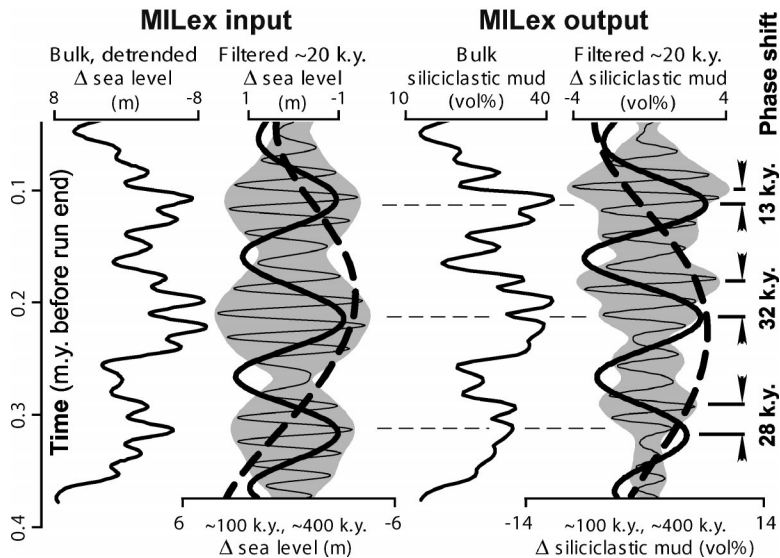
Figure 5. Selected input and output parameters of MILex model. Note that amplitude modulation (AM) of output precession-derived signal (~20 k.y.) is distinctly phase shifted relative to original AM of input ~20 k.y. signal. In accordance with conceptual model (Fig. 4), maxima in output ~20 k.y. amplitudes coincide with intervals of ~100 k.y. (thick solid line) decline in siliciclastic flux, and are further amplified upon ~400 k.y. (thick dashed line) decline in siliciclastic flux. Similarly, maximum amplitude of output ~100 k.y. signal (~0.11 m.y. before run end) formed during ~400 k.y. decline in siliciclastic flux.

The simulations suggest that a systematic amplitude distortion is inherent in dilution-driven hemipelagic cycles controlled by composite oscillations in relative sea level. Changes in the capacity of the nearshore part of the source siliciclastic depositional system due to LP changes in relative sea level systematically modulate the amplitudes of nested, SP transgressive-regressive changes and corresponding changes in offshore siliciclastic flux. As a result, the stratigraphic record of non-Milankovitch cycles (e.g., quasi-periodic faulting) can exhibit AM, which, in noisy stratigraphic records, could resemble Milankovitch-driven AM. Alternatively, depositional processes can distort Milankovitch-controlled AM by changing the phase and coherence of the SP amplitude envelope (e.g., envelope of the precession-driven signal) relative to the modulating signal (e.g., eccentricity; Fig. 5). These processes act at multiple temporal scales (Fig. 5) and represent an important aspect to consider in cyclostratigraphic studies of dilution-affected hemipelagic rhythmites (e.g., Bridge Creek Limestone Member and Niobrara Formation, Western Interior Basin; Lower Chalk of southeastern England; Cenomanian of southern France). Mismatch between theoretical and recorded AM patterns identified in hemipelagic strata by, e.g., Weedon and Jenkyns (1999) and Palike et al. (2001) might be attributable to distortion of the orbital signal via these depositional processes.

Sea-level–driven amplitude distortions tend to generate the highest amplitude of SP (e.g., 20 k.y.) cycles of siliciclastic flux during intervals of LP (e.g., 100 k.y., 400 k.y.) rise in relative sea level and associated decline in siliciclastic flux. This phase signature could be employed to recognize the record of relative sea-level change in hemipelagic rhythmites and thus, e.g., identify possible orbital forcing of eustasy in poorly understood intervals such as the greenhouse Cretaceous.

Stratigraphic records that allow a direct comparison of relative sea-level changes and T-R fluctuations with coeval hemipelagic cyclicity—e.g., the Cenomanian–Turonian of the Western Interior Basin (Laurin and Sageman, 2001) and the upper Turonian of the Bohemian Cretaceous Basin (Laurin and Uličný, 2004)—should provide an independent test of the preceding concept.

REFERENCES CITED

Boylan, A.L., Waltham, D.A., Bosence, D.W.J., Badenas, B., and Aurell, M., 2002, Digital rocks: Linking forward modelling to carbonate facies: Basin Research, v. 14, p. 401–415.

Hardy, S., and Waltham, D., 1992, Computer modeling of tectonics, eustasy, and sedimentation using the Macintosh: Geobyte, v. 7, p. 42–52.

Helland-Hansen, W., and Martinsen, O.J., 1996, Shoreline trajectories and sequences; description of variable depositional-dip scenarios: Journal of Sedimentary Research, v. 66, p. 670–688.

Herbert, T.D., 1994, Reading orbital signals distorted by sedimentation; models and examples, in de Boer, P.L., and Smith, D.G., eds., Orbital forcing and cyclic sequences: International Association of Sedimentologists Special Publication 19, p. 483–507.

Howell, P., 2001, ARAND time series and spectral analysis package for the Macintosh, Brown University: IGBP PAGES/World Data Center for Paleoclimatology Data Contribution Series 2001–044: Boulder, Colorado, NOAA/NGDC Paleoclimatology Program.

Imbrie, J., and 18 others, 1993, On the structure and origin of major glaciation cycles: 2. The 100,000-year cycle: Paleoceanography, v. 8, p. 698–735.

Laskar, J., 1990, The chaotic motion of the solar system: A numerical estimate of the chaotic zones: Icarus, v. 88, p. 266–291.

Laurin, J., and Sageman, B.B., 2001, Tectono-sedimentary evolution of the western margin of the Colorado Plateau during the latest Cenomanian and early Turonian, in Erskine, M.C., et al., eds., The geologic transition: High plateaus to Great Basin: Utah Geological Association Publication 30, p. 57–74.

Laurin, J., and Uličný, D., 2004, Controls on a shallow-water hemipelagic carbonate system adjacent to a siliciclastic margin; example from late Turonian of central Europe: Journal of Sedimentary Research, v. 74, p. 697–717.

Liu, K., Liang, T.C.K., Paterson, L., and Kendall, C.G.S, 1998, Computer simulation of the influence of basin physiography on condensed section deposition and maximum flooding: Sedimentary Geology, v. 122, p. 181–191.

Paillard, D., Labeyrie, L., and Yiou, P., 1996, Macintosh program performs time-series analysis: Eos (Transactions, American Geophysical Union), v. 77, p. 379.

Palike, H., Shackleton, N.J., and Roehl, U., 2001, Astronomical forcing in late Eocene marine sediments: Earth and Planetary Science Letters, v. 193, p. 589–602.

Plint, A.G., 1991, High-frequency relative sea-level oscillations in Upper Cretaceous shelf clastics of the Alberta foreland basin: Possible evidence for a glacio-eustatic control?, in MacDonald, D.I.M., ed., Sedimentation, tectonics and eustasy: International Association of Sedimentologists Special Publication 12, p. 409–428.

Ripepe, M., and Fischer, A.G., 1991, Stratigraphic rhythms synthesized from orbital variations, in Franseen, E.K., et al., eds., Sedimentary modeling; Computer simulations and methods for improved parameter definition: Kansas State Geological Survey Bulletin 233, p. 335–344.

Ross, W.C., Watts, D.E., and May, J.A., 1995, Insights from stratigraphic modeling: Mud-limited versus sand-limited depositional systems: American Association of Petroleum Geologists Bulletin, v. 79, p. 231–258.

Weedon, G.P., and Jenkyns, H.C., 1999, Cyclostratigraphy and the Early Jurassic time scale: Data from the Belemnite Marls, Dorset, southern England: Geological Society of America Bulletin, v. 111, p. 1823–1840.